

Provided for non-commercial research and education use.
Not for reproduction, distribution or commercial use.



This article appeared in a journal published by Elsevier. The attached copy is furnished to the author for internal non-commercial research and education use, including for instruction at the author's institution and sharing with colleagues.

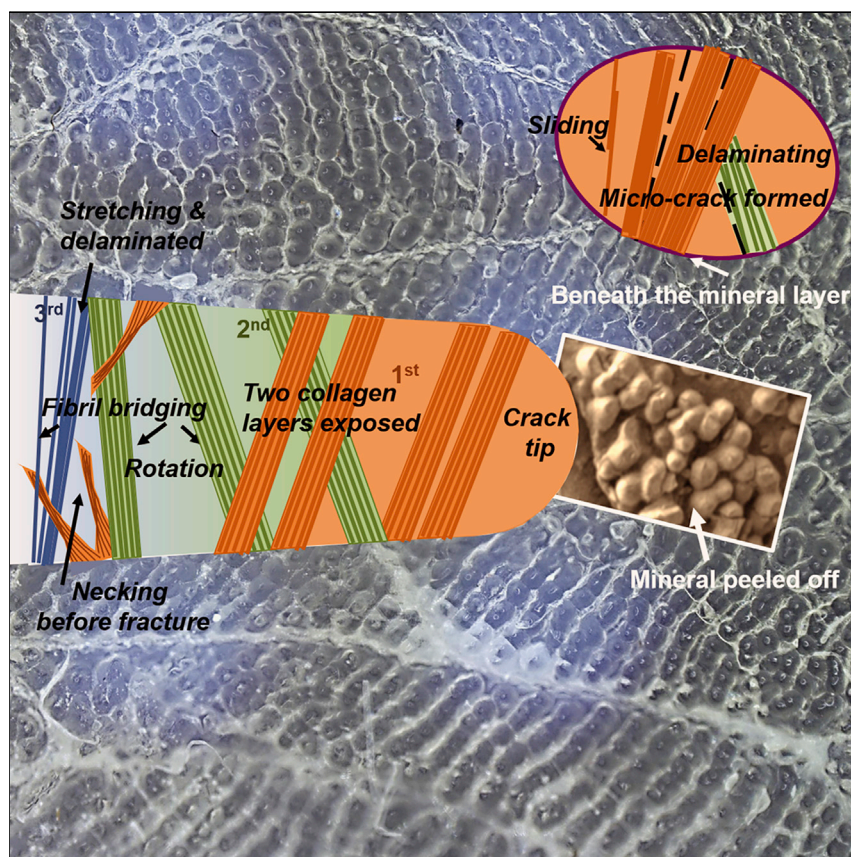
Other uses, including reproduction and distribution, or selling or licensing copies, or posting to personal, institutional or third party websites are prohibited.

In most cases authors are permitted to post their version of the article (e.g. in Word or Tex form) to their personal website or institutional repository. Authors requiring further information regarding Elsevier's archiving and manuscript policies are encouraged to visit:

<http://www.elsevier.com/authorsrights>

Article

Arapaima Fish Scale: One of the Toughest Flexible Biological Materials



Many fish scales are efficient natural dermal armors that protect fish from predators without impeding their flexibility; therefore, mimicking their design in synthetic materials may lead to improved lightweight armor. The scales of arapaima fish are particularly effective because they enable its survival in piranha-infested waters. With a highly mineralized outer layer to resist penetration and a tougher lower layer with a twisted arrangement of mineralized collagen fibrils to absorb deformation, these scales are one of nature's toughest flexible materials.

Wen Yang, Haocheng Quan,
Marc A. Meyers, Robert O.
Ritchie

roritchie@lbl.gov

HIGHLIGHTS

Arapaima fish have tough penetration-resistant scales for predator protection

The collagenous substrate is tough via deformation mechanisms acting in concert

Synergetic stretching, rotation, bridging, and sliding mechanisms delocalize damage

Fracture tests indicate the scales are one of nature's toughest flexible materials



Understanding

Dependency and conditional studies on material behavior

Yang et al., Matter 1, 1557–1566
December 4, 2019 © 2019 Elsevier Inc.
<https://doi.org/10.1016/j.matt.2019.09.014>



Article

Arapaima Fish Scale: One of the Toughest Flexible Biological Materials

Wen Yang,^{1,3} Haocheng Quan,^{1,3} Marc A. Meyers,¹ and Robert O. Ritchie^{2,4,*}

SUMMARY

For fish scales to provide protection from predators without severely compromising mobility, they must be lightweight, flexible, and tough. The arapaima fish scale is a superb example of this, enabling its survival in piranha-infested lakes of the Amazon. These elasmoid scales comprise two layers: a laminate composite of parallel collagen fibrils arranged in a *Bouligand*-like pattern and a highly mineralized surface layer that prevents initial penetration damage. Here, we measure its *J*-integral fracture toughness and find that the crack-growth toughness is $\sim 100\text{--}200\text{ kJ}\cdot\text{m}^{-2}$, representing a very high fracture resistance for a natural material. This toughness results from multiple deformation mechanisms acting in concert in the twisted plywood structure of the scale, involving the collagenous lamellae at varying orientations retarding crack advance through stretching, reorientation, delamination and shear, and fracture. The toughness values obtained for the arapaima scales indicate that they are among the toughest of nature's flexible biological materials.

INTRODUCTION

Hardness and strength are important material properties but only describe mechanical performance imperfectly. A fundamental parameter that bridges these two concepts is the fracture toughness, which is the ability of a material to resist the propagation of cracks and/or flaws when loaded.¹ This is especially true for structural materials where the toughness becomes the overriding property.² The same applies to biological materials that are subjected to extreme loads.^{3–9} The dermal armor of fish is a splendid example where the toughness is essential.^{10–17}

Arapaima gigas are a large Amazonian fish (weighing up to 150 kgf) living primarily in seasonal lakes infested with ferocious piranhas.¹⁸ The fish is covered with elasmoid scales composed of a mineralized outer layer that provides penetration resistance through its hardness and a more ductile inner collagenous lamellae layer, following a *Bouligand*-type pattern, that confers deformability to accommodate excessive deformation; the result is a tough scale with exceptional resistance to cracking from penetration by the teeth of predators. The outer layer of the arapaima scale is highly mineralized, containing ridges and protrusions in small divided areas ($\sim 3\text{ mm}^2$), which are thought to improve the flexibility of the scales, thereby generating a "ductile" ceramic.¹⁹ A cross-section of the arapaima scale, shown in Figure 1A₁ with the thickness of the outer and inner layers indicated, shows that each lamella in the inner layer is composed of parallel collagen fibrils in different orientations; two lamellae are imaged by transmission electron microscopy (TEM) in Figures 1A₂–1A₄. Collagen fibrils in two adjacent lamellae, perpendicular and parallel to the observation plane, are displayed in Figures 1A₃ and

Progress and Potential

Biological materials science involves the study of natural materials to understand their structures and find the origins of the properties that underlie their functionality. This knowledge in turn can then be used to design improved synthetic materials with the inspiration of nature.

Fish scales are an excellent example because they are highly efficient natural dermal armors that protect fish from predators without impeding their flexibility. Thus, mimicking their design in engineering materials can lead to improved lightweight armor materials. The scales of the *Arapaima gigas* represent especially effective protection, because they enable the survival of this large fish in piranha-infested waters. By means of a highly mineralized outer layer to resist penetration and a softer yet far tougher lower layer, involving a twisted plywood structure of mineralized collagen fibrils to absorb excessive deformation, we show that these scales are one of the toughest flexible materials in nature.



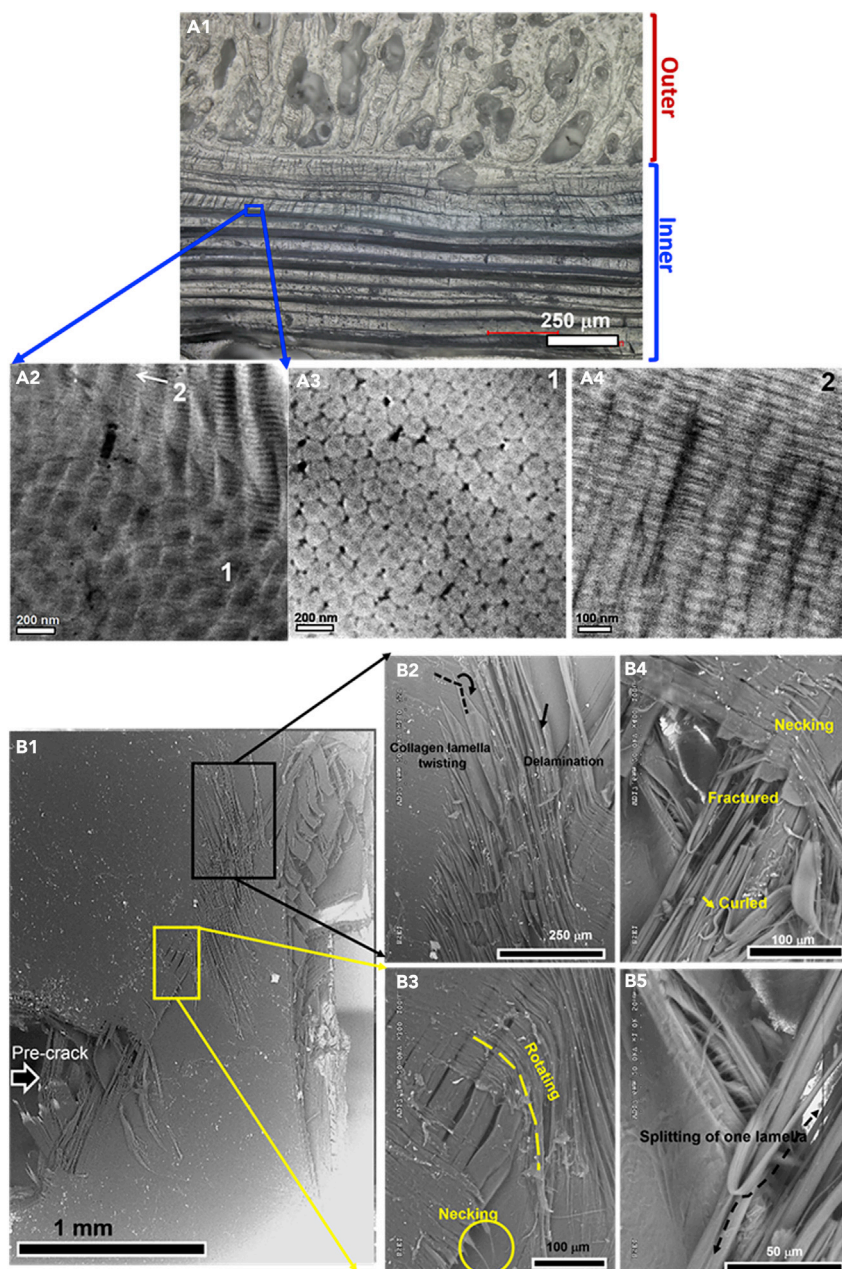


Figure 1. Structure and Deformation Mechanisms in Arapaima Scales

(A) Structure of the arapaima scale. (A₁) Cross-section of the arapaima scale indicating the thickness of the outer and inner layers; (A₂) transmission electron micrographs showing collagen fibrils in two adjacent lamellae: 1, perpendicular to the plane; 2, parallel to the plane; (A₃ and A₄) higher magnification views of regions 1 and 2.

(B) Deformation response is dependent on the orientation of the lamella, and crack propagation paths differ from one lamella to another; (B₁) overall view of the crack front region, (B₂) lamellar delamination and twisting, (B₃) rotating and bending of fibril packets in lamellae, (B₄) necking and fracturing of fibril packets, (B₅) separation of fibril packets by splitting.

1A₄. Figure 1A₂, taken at the interface between two lamellae, illustrates two orientations. The fibrils have a characteristic diameter of ~ 100 nm and are organized in a quasi-hexagonal arrangement due to their tight packing, which comprise the

¹Materials Science & Engineering Program, Department of Mechanical & Aerospace Engineering, and Department of NanoEngineering, University of California San Diego, La Jolla, CA 92093, USA

²Department of Materials Science & Engineering, University of California Berkeley, Berkeley, CA 94720, USA

³These authors contributed equally

⁴Lead Contact

*Correspondence: roritchie@lbl.gov
<https://doi.org/10.1016/j.matt.2019.09.014>

lamellae, each $\sim 50 \mu\text{m}$ thick. Although the structure of arapaima scales and their mechanical properties, notably hardness, modulus, strength, ductility, puncture resistance, and adaptive mechanisms of structural evolution during tensile load, have been well established,^{19–22} their fracture toughness value, i.e., the stress intensity or energy required to fracture them in the presence of a worst-case flaw, is still lacking quantitative analysis. Dastjerdi and Barthelat¹² applied fracture-mechanics measurements to estimate the toughness of elasmoid scales, specifically for striped bass, and showed that these scales were tough flexible materials. In this communication, we report a new design for measuring a more realistic fracture toughness of the arapaima fish scale and confirm that it is among the toughest flexible biological materials. Our study may also provide inspiration for the process of the mechanical testing of other biological materials. We note here that there are two primary principal fracture-mechanics parameters used to measure the toughness, namely the linear-elastic “crack-driving force,” K_c , and a corresponding nonlinear-elastic energy parameter, J_c . They can be related through the mode I J/K equivalence relationship: $J_c = K_c^2/E'$, where $E' = E$ (Young’s modulus) under plane-stress conditions and $E/(1 - \nu^2)$ in plane strain (ν is Poisson’s ratio).²³ However, because of the small size of the scales and their inherent plasticity, which tend to invalidate a linear-elastic fracture-mechanics approach, our focus is on determining a nonlinear-elastic J_c fracture toughness, which is a more appropriate methodology to evaluate the fracture resistance of these scales.

The (mode I) fracture toughness can be obtained by creating an artificial (worst-case) crack in a material and then loading it in tension. If the flaw resists further cracking, the material can be considered as tough. Despite the simplicity of this methodology, testing biological materials can be somewhat more problematic. Thus, it was necessary to develop a new compact-tension testing fixture to evaluate the fracture toughness of the arapaima scales because of their specific geometry and related mechanical effects. Unlike that used by Dastjerdi and Barthelat,¹² our fixture was designed to not constrain the crack by enabling the two ends of the grips to rotate freely under increased loading but to still provide the bending plus tension loading characteristic of the natural fish scale geometry. Figure 2A shows the apparatus design; additional details as well as our methods of analysis are provided in the Experimental Procedures. Specifically, the testing of the scales presents two challenges: (1) the perforation of the scales to introduce the loading pins as well as the tears in scales during testing, and (2) the scale is subjected to out-of-plane buckling during the application of the external force, which causes combined mode I (tensile) plus mode III (anti-plane shear) loading of the crack. To avoid tearing at the pins during the test, the perforations on the scale to insert loading pins were replaced by an adaptor rigidly attached to the scales by two screws and having the ability to rotate freely upon loading, thus eliminating the need for constrained loading. To avoid mixed-mode loading, we used two lateral plates to sandwich the sample in a manner that minimizes out-of-plane buckling. Both solutions are shown in Figures 2A and 2B.

There are two modes of loading that can cause damage to the fish scale:

- a. Flexure with compression in the external surface and tension in the internal surface. It would be extremely difficult to prepare a toughness sample along the thickness direction because the crack length has to be very small, a fraction of a millimeter, as the scale thickness is $\sim 1.5 \text{ mm}$. In this geometry, the crack propagation direction is perpendicular to the lamellae.

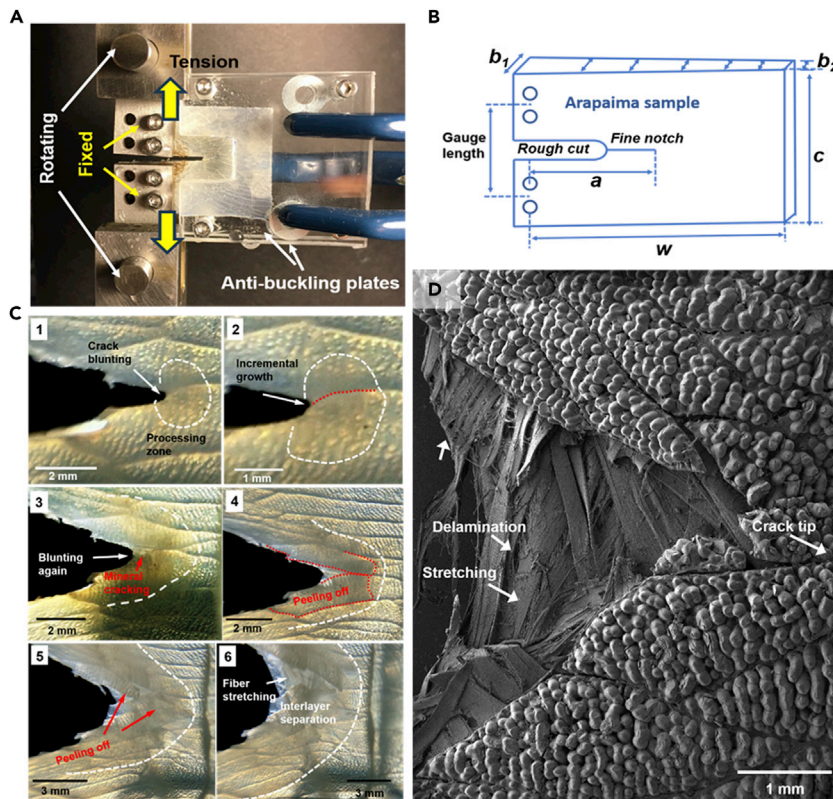


Figure 2. Experimental Setup and Crack-Tip Behavior

(A) Fracture toughness measurement setup showing platens with rotation pins attached to sample ends. The sample is sandwiched between four steel platens by screws; the latter are connected by loading pins to the tensile testing machine, allowing for free rotation as the arrow indicates. A pair of anti-buckling guide plates prevents the sample from bending out of plane during the test.

(B) Sample design and dimensions.

(C) Six successive views of the stages of crack-tip behavior during the fracture toughness test. The white dashed line shows the process zone (see text).

(D) Configuration of lamellae at the crack front; the cracking of the mineralized layer causes separation at an early stage. The major contribution to the toughness results from stretching, rotation, delamination, and fracture processes occurring in the compliant collagen lamellae.

- b. Tension loading of the scale with the crack propagation direction parallel to the lamellae. This orientation simulates the damage produced by a tooth that penetrates through the scale and is pushed further in, creating a void that could be transformed into a crack if the toughness is not sufficient. This is the situation that we are addressing in the current loading configuration, similar to the one described by Dastjerdi and Barthelat.¹²

Indeed, in our previous study,¹⁹ we determined the penetration effect on the arapaima fish scales and discovered that the *Bouligand* structure could develop similar toughening mechanisms to protect the scale against both penetration and tensile loads. Here, we aim to use a natural pre-cracked fish scale (mimicking the pre-damage created by predators) to illustrate how the damaged scales can still carry load and provide protection from predators. We show that the lamellae are powerful crack inhibitors because of their *Bouligand* arrangement.

RESULTS AND DISCUSSION

Using this technique, the sequence of deformation, imaged using optical microscopy at the crack tip in a moist arapaima scale, is shown in Figure 2C; a video of this deformation sequence, taken in real time during the toughness test, is shown in Video S1. The white dashed line shows the boundary of the process zone, which was estimated by the change in coloration of the mineral layer, produced by the separation from the collagenous lamellae when the latter undergo substantial non-elastic deformation. As Dastjerdi and Barthelat¹² also remarked, the mineral undergoes whitening when this occurs. This region has a dimension of $\sim 1\text{--}4$ mm and expands with the evolution of loading. Because of its greater hardness and lesser ductility, the mineral first cracks at the surface and gradually peels off from the lamellar *Bouligand* layers. Further increase in the applied load causes an enlargement in the area of the separated mineral layer with more mineral fragments peeling off. The advanced design of divided areas in the mineral layers results in a local peeling-off with other areas remaining intact. The crack tip undergoes blunting, advance, and re-blunting as the lamellae in different orientations deform and reorient; finally interlayer separation occurs in collagenous lamellae. The observation of crack-tip behavior suggests that the arapaima scale can undergo high loads and significant deformation without catastrophic failure. The fractured mineral layer and the exposed blunted lamellae are shown in greater detail in Figure 2D. The distinct behavior of the two layers is clearly apparent; both the crack tip in the mineral layer (as shown by the arrow) and the significant increase in the crack-tip radius due to blunting in the collagenous layer can be clearly seen. Whereas the crack advances readily in the mineral, the collagen lamellae resist the advance through the mechanisms of deformation from fiber reorientation, separation, delamination, shear, twist and fracture. Based on this synergy of multiple deformation mechanisms that act to resist fracture, the question is what magnitude of fracture toughness is actually induced in this excellent damage-tolerant material.

This question is addressed by a nonlinear-elastic fracture-mechanics analysis method based on our J -integral fracture toughness testing of moist arapaima scales, the experimental and analysis details of which are provided in the Experimental Procedures. Note that we elected to not present the simpler linear-elastic fracture-mechanics stress-intensity K -based toughness analysis because the scales were too small and displayed too much plasticity (the flow stress of the scale in the transverse direction is $\sigma_o \sim 22$ MPa¹⁹) to satisfy the small-scale yielding criterion for the validity of K -based crack-tip stress and displacement fields accordingly to the ASTM Standard E1820 for fracture toughness measurement.²³ Moreover, such linear-elastic measurements do not account for the important contribution of plastic deformation, which invariably plays a major role in enhancing the toughness of biological materials.²⁴ Further discussion on our toughness measurements are given in the Experimental Procedures.

Figure 3A shows the results of our measurements of the crack-resistance curves in terms of J as a function of stable crack advance, Δa ; the R-curve data for moist arapaima fish scales measured on five different samples are plotted, where an increase in J is required to advance the crack stably. Based on these R-curves where stable cracking takes place for up to $\Delta a \sim 6$ mm, a maximum (plateau) J_{\max} value of $\sim 100\text{--}200$ kJ $\cdot\text{m}^{-2}$ can be deduced for the stable crack growth. This value does not satisfy a condition of plane strain, but this is not relevant because it represents the toughness of actual ~ 1 -mm-thick scales. However, it definitively represents a valid J measurement, as discussed in the Experimental Procedures, and clearly

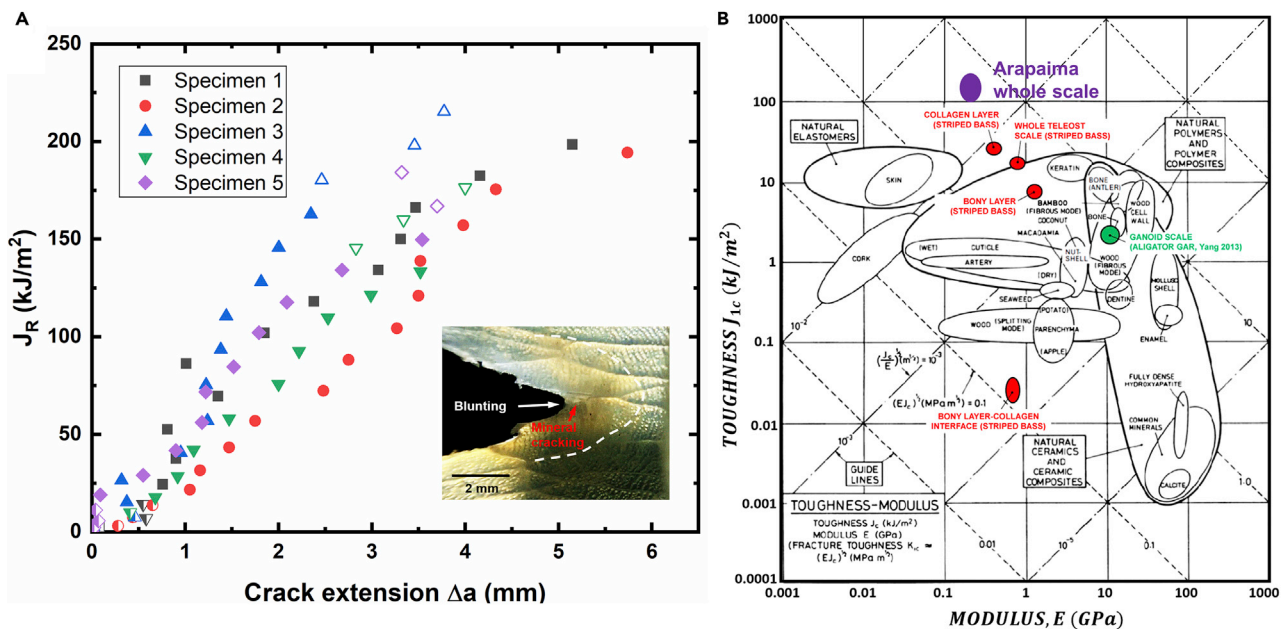


Figure 3. Fracture Toughness of Arapaima Scales

(A) Nonlinear-elastic fracture-mechanics J -based measurements of the crack resistance (R -curves) for wet arapaima scales in the form of J_R as a function of crack extension Δa for five representative samples. Inset shows the crack opening and associated crack blunting.

(B) Ashby plot of fracture toughness (J_{IC}) versus elastic modulus (E) showing a comparison with other biological materials, including striped bass¹² and ganoid scale.²¹ The arapaima scales show high toughness of ~ 100 – 200 $\text{kJ}\cdot\text{m}^{-2}$. Note in (A) that the crack-initiation toughness, where $\Delta a \rightarrow 0$, can be extremely low; this is because the highly mineralized layer at the surface of the scale (where our crack extension measurements are made) can sometimes break almost immediately on loading. These data are represented by half-open/half-solid symbols. Also, the open symbols on some of the R -curves at longer crack extensions were not considered for analysis because this is where we observed some degree of buckling as the longitudinal (load-line) displacements of the sample became too large (typically exceeding ~ 10 mm) for the anti-buckling plates to work effectively).

demonstrates the exceptional crack-growth toughness of the arapaima scales. In energy terms, this toughness value is higher by one order of magnitude than that of Dastjerdi and Barthelat;¹² however, they used a constrained testing configuration which, as they themselves state, can severely underestimate the toughness. In terms of a stress-intensity value, using the Young's modulus measured for the arapaima scale in the relevant transverse direction of $E \sim 210$ MPa,¹⁹ our measured J -based fracture toughness of 200 $\text{kJ}\cdot\text{m}^{-2}$ translates to an approximate K -based crack-growth fracture toughness of ~ 6.4 $\text{MPa}\cdot\text{m}^{1/2}$.

In respect to comparisons with the measurements of the toughness of striped bass scales,¹² another significant difference between these and the current arapaima fish is the thickness of the lamellae; the lamellae thickness for the arapaima fish is ~ 50 μm ,¹⁹ whereas it is only 5 μm for the striped bass.¹² The thicker lamellae can not only provide higher strength due to the larger number of collagen fibrils but also involve the breakage of more interfaces during the plastic deformation, which is vital for toughening the material.

The shape of the R -curves of the tougher arapaima scales displays a progressively increasing toughness over a range of stable crack extensions of $\Delta a \sim 1.5$ – 5 mm before reaching the ~ 100 – 200 $\text{kJ}\cdot\text{m}^{-2}$ "plateau" (Figure 3A). The initial toughness can be seen to be quite low, with some R -curves displaying an S shape, which can be related to the rapid initial cracking of the brittle mineral surface layer (which can bias our crack length measurements because they are made at the surface). Once this surface layer fails, however, the resultant sequence of mechanisms of extensive plastic



deformation in the collagen layers serves to increasingly resist crack extension with a consequent increase in crack-growth toughness. Over $\sim 5\text{--}6$ mm of such crack extension, the maximum (valid) crack extension capacity of our sample is exceeded; at this stage in some of the samples, some degree of out-of-plane buckling was detected (these invalid data points are delineated by open symbols on the relevant R-curves). Nevertheless, considering only the valid data points under this condition, we are able to measure a reliable value for the crack-growth toughness of moist arapaima fish scales of J_{\max} values between ~ 100 and $200 \text{ kJ}\cdot\text{m}^{-2}$ in our five tested samples.

These results are plotted on an Ashby map²⁵ for the J -based toughness as a function of modulus for a number of important biological materials, including other fish scales such as those of the striped bass scale (Figure 3B). The ellipsis for the arapaima encompasses our measured crack-growth toughness values between 100 and $200 \text{ kJ}\cdot\text{m}^{-2}$. The arapaima and striped bass fish scales are the toughest flexible biological materials in the plot. As noted above, the toughness of the striped bass scales was measured by Dastjerdi and Barthelat,¹² who correctly attributed the toughening mechanisms to their intricate and ingenious hierarchical structure.

For the arapaima scale in the present study, the principal deformation processes taking place ahead of the crack tip were imaged *in situ* during loading in the scanning electron microscope and are shown in Figure 1B; in addition, Video S2 provides real-time observations of these crack-tip processes. These images specifically highlight how each individual lamella undergoes a different sequence of deformation processes (which incidentally makes it difficult to precisely define the actual crack front). This is shown in the overall view of Figure 1B₁ and in detail in Figures 1B₂–1B₅.

To focus on this synergy of toughening mechanisms, we can examine Figures 1B₂–1B₅ in turn. When the collagen fibrils are perpendicular to the crack front, they provide maximum resistance; indeed, in this orientation, crack advance requires their fracture. At oblique angles, there are significant sliding and reorientation of these fibrils before fracture. This can cause the crack to undergo a change in path and can, at the specific lamellae, change the character of its local trajectory from pure mode I (tension) to mixed modes I + II (tension + in-plane shear). When the crack is aligned with the fibrils, it advances by interfibrillar separation. The overall view of the crack front region is magnified in Figure 1B₁ which clearly shows such rotation and bending of fibril packets within the lamellae. Figure 1B₂ shows delamination and collagen lamellae twisting, a mechanism of delocalizing the crack front by spreading it over a larger area. At this last stage before failure, the most serious deformation is located at either the crack front or the other edge of the sample. In between, most collagen fibers undergo rotation with some fractured with necking, as shown in Figure 1B₃. More severe fractures of fibril packets with curled collagen fibrils can be seen in Figure 1B₄; the separation of fibril packets by splitting is illustrated in Figure 1B₅. As the crack advances, the collagenous lamellae in different orientations coordinate to reach an extreme state for the crack resistance.

This sequence of toughening mechanisms was confirmed by observations during *in situ* tension testing of wet scales in an environmental scanning electron microscope. Rotating, stretching, delamination, necking, surface twisting of lamellae, and before failure splitting of one lamella, were all observed. Indeed, to some extent, all the lamellae in the *Bouligand* structure experience similar mechanisms, with a clear separation from the outer layer, although under such hierarchical deformation, including separation between the lamellae in the thickness direction and the delamination of the collagen fibers within one lamella, the scale sample was still under tension and

did not fail catastrophically. Such mechanisms are the result of accommodation and cooperation of the collagen lamellae. Some of these processes have been identified previously for arapaima fish scales,^{19,22} but this is the first time that an evaluation of their sequence during the crack opening, with the identification of several new mechanisms including sublayer twisting and splitting, has been made for the collagenous *Bouligand* structure. All these toughening mechanisms act in concert to provide for the outstanding deformability of arapaima scales and engender their remarkable toughness, making them highly damage-tolerant, armor materials.

Conclusions

In summary, the R-curve toughness of arapaima fish scales was measured to be as high as $200 \text{ kJ}\cdot\text{m}^{-2}$ (equivalent to a stress-intensity toughness of on the order of $6.4 \text{ MPa}\cdot\text{m}^{1/2}$), which represents an exceptional fracture toughness associated with a synergy of deformation mechanisms acting in concert in the lamellae of tightly packed parallel collagen fibrils. Specifically, the *Bouligand*-type organization of the collagen fibrils in the arapaima scales provides close to in-plane isotropy to the scale, whereas each lamella is strongly anisotropic; thus, the hierarchical toughening mechanisms dissipate energy within the sub-layers through collagen lamellar separation, collagen fibrillar bridging, sliding, and delamination. Although similar mechanisms have been observed in the fish scales of striped bass,¹² the significantly higher toughness of the arapaima scales appears to be associated with the increased thickness of their lamellae layers and scale thickness itself, and to a higher degree of mineralization, a necessity for protection of the arapaima from piranha attacks in the Amazon basin.

EXPERIMENTAL PROCEDURES

Fracture Toughness Testing Procedures

Due to the thin-sheet like geometry of arapaima scale, conventional compact-tension C(T) sample fracture toughness measurement (ASTM E1820²³) is difficult. Instead, thin-sheet compact samples (modified 1T plan samples) were extracted from scales of juvenile arapaima ($\sim 40 \text{ kg}$). The thickness of these scales, which is on the order of 1 mm, is not uniform; therefore, measurement of the thickness, B , involved the average taken at similar positions on each sample. The in-plane dimensions of the scales were between 50 and 120 mm; consequently, these dimensions followed the conventional 1T compact geometry provided in the ASTM Standard,²³ specifically with $W \sim 50 \text{ mm}$. To provide a pre-notch, a rough cut was first introduced along the longitudinal direction of the scale using a low-speed diamond saw and then sharpened using a sharp razor blade to a crack length-to-sample width ratio, a/W , of ~ 0.5 . Four through-thickness holes were prepared using Dremel, with two on each side of the pre-notch, as indicated in Figure 2B, resulting in a gauge length of 12.5 mm. The samples were tightened to the steel plates by screws connected to the Instron with pins to enable free rotation. Testing was performed on five individual wet scales in displacement control on an Instron 3342 mechanical testing machine (Instron Corp. Norwood, MA, USA) applied to the transverse direction of the fish scales with a load cell of 500 N at a displacement rate of 0.06 mm/min. Before testing, the arapaima fish scale samples were stored in fresh water.

To fully quantify the crack-growth fracture toughness of the arapaima scales and to incorporate the important role of plasticity in generating the toughness, as noted above we used nonlinear-elastic fracture-mechanics methods and performed measurements of the J -based fracture toughness, J_{max} , and the full $J_R(\Delta a)$ R-curves, in accordance with ASTM Standard E1820.²³ The J -integral for sharply notched test specimens can be determined in terms of the sample thickness, B , and

uncracked ligament, b , ahead of the crack tip, i.e., $(W - a)$, from the following relationship:²³

$$J = \frac{\eta A_T}{Bb},$$

where A_T is the total area (elastic plus plastic) under the load versus load-line displacement curve integrated from the beginning (zero displacement) to a given displacement determined by a pertinent value of Δa , and η is the specimen geometry factor, given by $\eta = 2 + 0.522 b/W$. We have used the total (elastic + plastic) area under the load versus load-line displacement curve to compute the total J , although ASTM E1820²³ recommends that the elastic component J_{el} be determined by calculating K_c^2/E . In our experience, it is invariably difficult to accurately determine an elastic modulus E for biological materials, particularly flexible ones like fish scales. For this reason, we find it more reliable to estimate J_{el} from the elastic area under the load versus load-line displacement curve. This approach combines estimates of the contributions to the J -integral toughness from both elastic and plastic deformation, because separating them can be a more complicated issue for biological tissue.

Figure 3A shows the resulting rising $J_R(\Delta a)$ curve toughness data for moist arapaima fish scales. Although these fracture toughness measurements were not in plane strain because they pertain to actual arapaima scales, J -field validity was assured as $b > 10 J/\sigma_o$,²³ where σ_o ($= 21.9$ MPa) is the flow stress for the arapaima scales in the transverse direction,¹⁹ perpendicular to the direction of crack propagation. Accordingly, the $J_R(\Delta a)$ curves in Figure 3A can be regarded as an accurate representation of the nonlinear-elastic fracture toughness of these scales.

In Situ ESEM Observation under Tension Loading

Additional fracture testing on the wet scales was performed in tension under displacement control using an *in situ* Gatan MicroTest 2-kN bending stage mounted in a Hitachi S-4300SE/N (Hitachi America, Pleasanton, CA, USA) environmental scanning electron microscope (ESEM). Due to the limitation of the stage, the width of the sample was restricted to ~ 6 mm containing a sharpened ~ 2 mm long notch. These tests were performed at a loading speed of 0.1 mm/min to directly observe how the mechanisms of crack blunting and crack advance evolve in real time during the progress of the R-curve. Samples were tested moist with the ESEM operating under low-pressure mode (35 Pa) and the images derived using the back-scattered electron imaging mode.

Preparation and Imaging of TEM Samples

The arapaima scales were first immersion-fixed in 3% glutaraldehyde in 0.15 M sodium cacodylate buffer (pH 7.4) for 4 h, and then post fixed using 1% OsO₄ solution with 8% potassium ferrocyanide in 0.15 M sodium cacodylate buffer for 12 h at 4°C. The scales were subsequently stained with 2% aqueous uranyl acetate for 12 h and dehydrated with an ascending ethanol series (50%, 70%, 90%, and 100%), followed by a 1/1 ratio of 100% ethanol and 100% acetone and finally 100% acetone. Samples were then embedded in Spurr's low viscosity resin and polymerized at 60°C for 48 h. Samples were subsequently sectioned perpendicular to the scale surface to generate slices 80–200 nm thick using a Leica Ultracut UCT ultramicrotome (Leica, Wetzlar, Germany) and a Diatome diamond knife (Diatome, Hatfield, PA). The sections were then stained with 1% uranyl acetate for 10 min and Sato lead for 1 min. These samples were examined in an FEI Tecnai 12 TEM at 120 kV.

SUPPLEMENTAL INFORMATION

Supplemental Information can be found online at <https://doi.org/10.1016/j.matt.2019.09.014>.

ACKNOWLEDGMENTS

This research was supported by the Air Force Office of Scientific Research, under MURI grant AFSOR-FA9550-15-1-0009 to the University of California Riverside through subcontracts to UC San Diego and UC Berkeley. We thank Prof. Sergio Neves Monteiro for obtaining arapaima scales and Dr. Louis G. Malito for assistance with the fracture toughness experiments.

AUTHOR CONTRIBUTIONS

W.Y. and H.Q. performed the experiments under the supervision of M.A.M. and R.O.R. All authors contributed to the writing of the manuscript.

DECLARATION OF INTERESTS

The authors declare no competing interests.

Received: June 2, 2019

Revised: August 13, 2019

Accepted: September 13, 2019

Published: October 16, 2019

REFERENCES

- Ritchie, R.O. (2011). The conflicts between strength and toughness. *Nat. Mater.* 10, 817.
- Launey, M.E., and Ritchie, R.O. (2009). On the fracture toughness of advanced materials. *Adv. Mater.* 21, 2103–2110.
- Dirks, J.H., and Taylor, D. (2012). Fracture toughness of locust cuticle. *J. Exp. Biol.* 215, 1502–1508.
- Wu, J., Qin, Z., Qu, L., Zhang, H., Deng, F., and Guo, M. (2019). Natural hydrogel in American lobster: a soft armor with high toughness and strength. *Acta Biomater.* 88, 102–110.
- Wang, B., Sullivan, T.N., Pissarenko, A., Zaheri, A., Espinosa, H.D., and Meyers, M.A. (2019). Lessons from the ocean: Whale Baleen fracture resistance. *Adv. Mater.* 31, 1804574.
- Porter, D., Guan, J., and Vollrath, F. (2013). Spider silk: super material or thin fibre? *Adv. Mater.* 25, 1275–1279.
- Pereira, B.P., Lucas, P.W., and Swee-Hin, T. (1997). Ranking the fracture toughness of thin mammalian soft tissues using the scissors cutting test. *J. Biomech.* 30, 91–94.
- Dirks, J.H., and Taylor, D. (2012). Veins improve fracture toughness of insect wings. *PLoS One* 22, e43411.
- Bechtle, S., Özcoban, H., Yilmaz, E.D., Fett, T., Rizzi, G., Lilleodden, E.T., Huber, N., Schreyer, A., Swain, M.A., and Schneider, G.A. (2012). A method to determine site-specific, anisotropic fracture toughness in biological materials. *Scr. Mater.* 66, 515–518.
- Murcia, S., McConville, M., Li, G., Ossa, A., and Arola, D. (2015). Temperature effects on the fracture resistance of scales from *Cyprinus carpio*. *Acta Biomater.* 14, 154–163.
- Barthelat, F. (2013). Science and engineering of natural materials: merging structure and materials. *J. Mech. Behav. Biomed. Mater.* 19, 1.
- Dastjerdi, A.K., and Barthelat, F. (2015). Teleost fish scales amongst the toughest collagenous materials. *J. Mech. Behav. Biomed. Mater.* 52, 95–107.
- Varshney, S., Zolotovskiy, E., Reichert, S., Li, Y.N., Oxman, N., Boyce, M.C., and Ortiz, C. (2014). Mechanical design rules of articulated fish scale armor. *Integr. Comp. Biol.* 54, E214.
- Varshney, S., Zolotovskiy, E., Li, Y.N., Boyce, M.C., Oxman, N., and Ortiz, C. (2013). Morphometric origins of biomechanical flexibility in fish armor. *Integr. Comp. Biol.* 53, E218.
- Browning, A., Ortiz, C., and Boyce, M.C. (2013). Mechanics of composite elasmoid fish scale assemblies and their bioinspired analogues. *J. Mech. Behav. Biomed. Mater.* 19, 75–86.
- Song, J., Ortiz, C., and Boyce, M.C. (2011). Threat-protection mechanics of an armored fish. *J. Mech. Behav. Biomed. Mater.* 4, 699–712.
- Bruet, B.J., Song, J., Boyce, M.C., and Ortiz, C. (2008). Materials design principles of ancient fish armour. *Nat. Mater.* 7, 748.
- Meyers, M.A., Lin, Y.S., Olevsky, E.A., and Chen, P.Y. (2012). Battle in the Amazon: Arapaima versus piranha. *Adv. Eng. Mater.* 14, B279–B288.
- Yang, W., Sherman, V.R., Gludovatz, B., Mackey, M., Zimmermann, E.A., Chang, E.H., Schaible, E., Qin, Z., Buehler, M.J., Ritchie, R.O., and Meyers, M.A. (2014). Protective role of *Arapaima gigas* fish scales: structure and mechanical behavior. *Acta Biomater.* 10, 3599–3614.
- Lin, Y.S., Wei, C.T., Olevsky, E.A., and Meyers, M.A. (2011). Mechanical properties and the laminate structure of *Arapaima gigas* scales. *J. Mech. Behav. Biomed. Mater.* 2011, 1145–1156.
- Torres, F.G., Troncoso, O.P., Nakamatsu, J., Grande, C.J., and Gomez, C.M. (2008). Characterization of the nanocomposite laminate structure occurring in fish scales from *Arapaima gigas*. *Mater. Sci. Eng. C* 28, 1276–1283.
- Zimmermann, E.A., Gludovatz, B., Schaible, E., Dave, N.K., Yang, W., Meyers, M.A., and Ritchie, R.O. (2013). Mechanical adaptability of the Bouligand-type structure in natural dermal armour. *Nat. Commun.* 4, 7.
- ASTM E1820-17a, (2017). Standard Test Method for Measurement of Fracture Toughness, ASTM International, West Conshohocken, PA, www.astm.org.
- Wegst, U.G., Bai, H., Saiz, E., Tomsia, A.P., and Ritchie, R.O. (2015). Bioinspired structural materials. *Nat. Mater.* 14, 23.
- Wegst, U.G.K., and Ashby, M.F. (2004). The mechanical efficiency of natural materials. *Philos. Mag.* 84, 2167–2186.